Electronic Supplementary Material (ESI) for Dalton Transactions.

SUPPLEMENTARY INFORMATION

Catalytic Metallodrugs Based on the LaR2C Peptide Target HCV SLIV IRES RNA

Martin James Ross[1], Seth S. Bradford[1], and J. A. Cowan[1,2]*

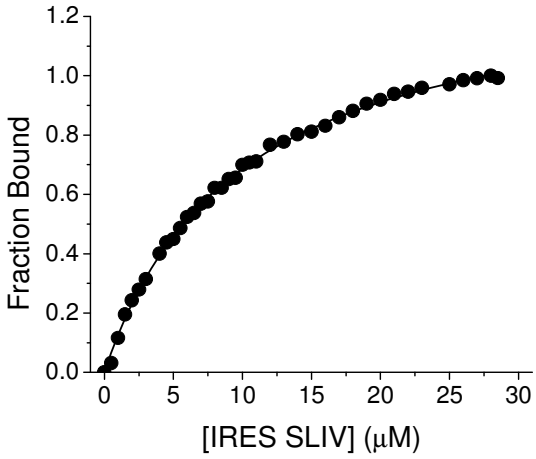

Figure SM1. Sample curve for binding of **3** to HCV IRES SLIV.

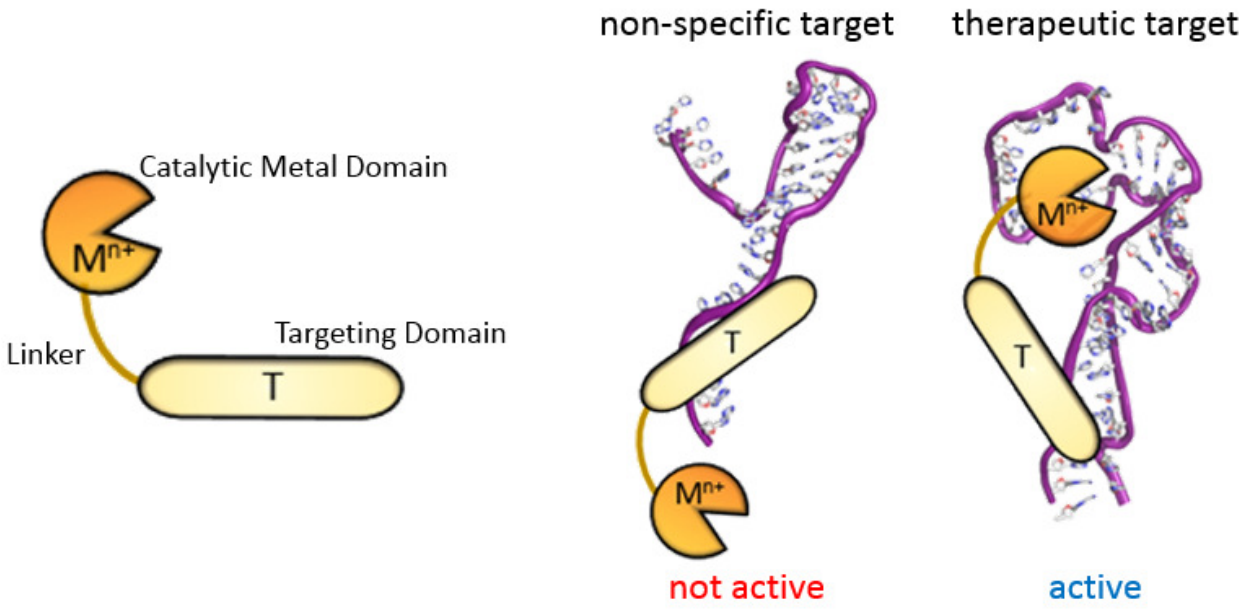

Figure SM2. The principle of the double-filter effect. (Left) graphical representation of a metallopeptide, depicting the catalytic metal domain (Cu-GGH moiety), and a generic targeting domain. (Middle and right) Binding of the targeting domain to two different RNAs. Even though both show binding, it is only the target on the right that is subject to irreversible cleavage and inactivation. This results from the positioning of the catalytic metal domain to perform chemistry on the target, but not on the alternative RNA. Use of lower concentrations will favor destruction of the therapeutic target and minimize reversible inhibition of the alternative RNA motif. In both of these cases the compound acts a reversible inhibitor until cleavage occurs.

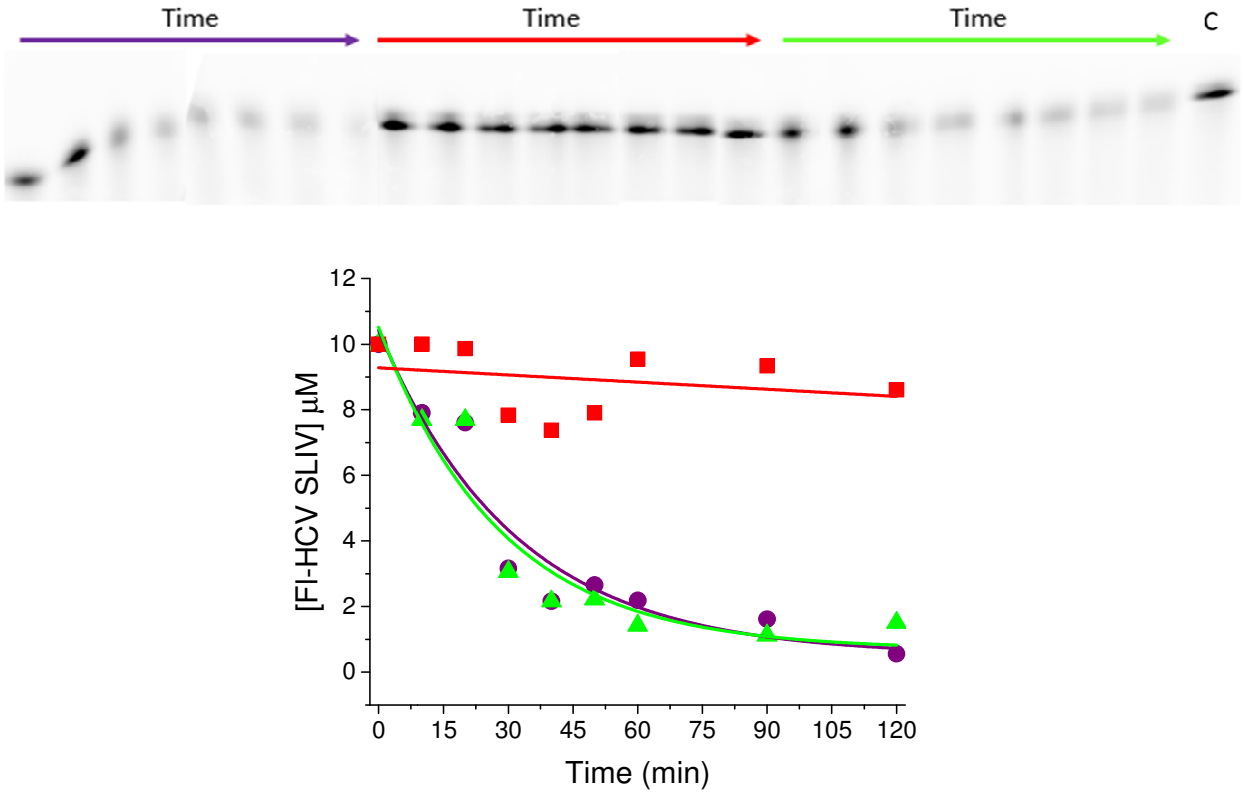

Figure SM3. Disappearance of full-length Fl-HCV-SLIV with **2**-Cu in the presence of ascorbic acid and hydrogen peroxide (top left, purple arrow), co-reagents only (top middle, red arrow), or **3**-Cu with co-reagents (top right, green arrow). The control lane (C) is shown on the on the far right. The time points for each data set were (left to right) 10, 20, 30, 40, 50, 60, 90, and 120 min. Reaction conditions included 10 µM RNA and 10 µM complex with 1 mM ascorbic acid and 1 mM hydrogen peroxide. (Bottom) Graphical representation of the disappearance of the full-length Fl-HCV SLIV, **2**-Cu (purple circles), **3**-Cu (green triangles), and co-reagents only (red squares).

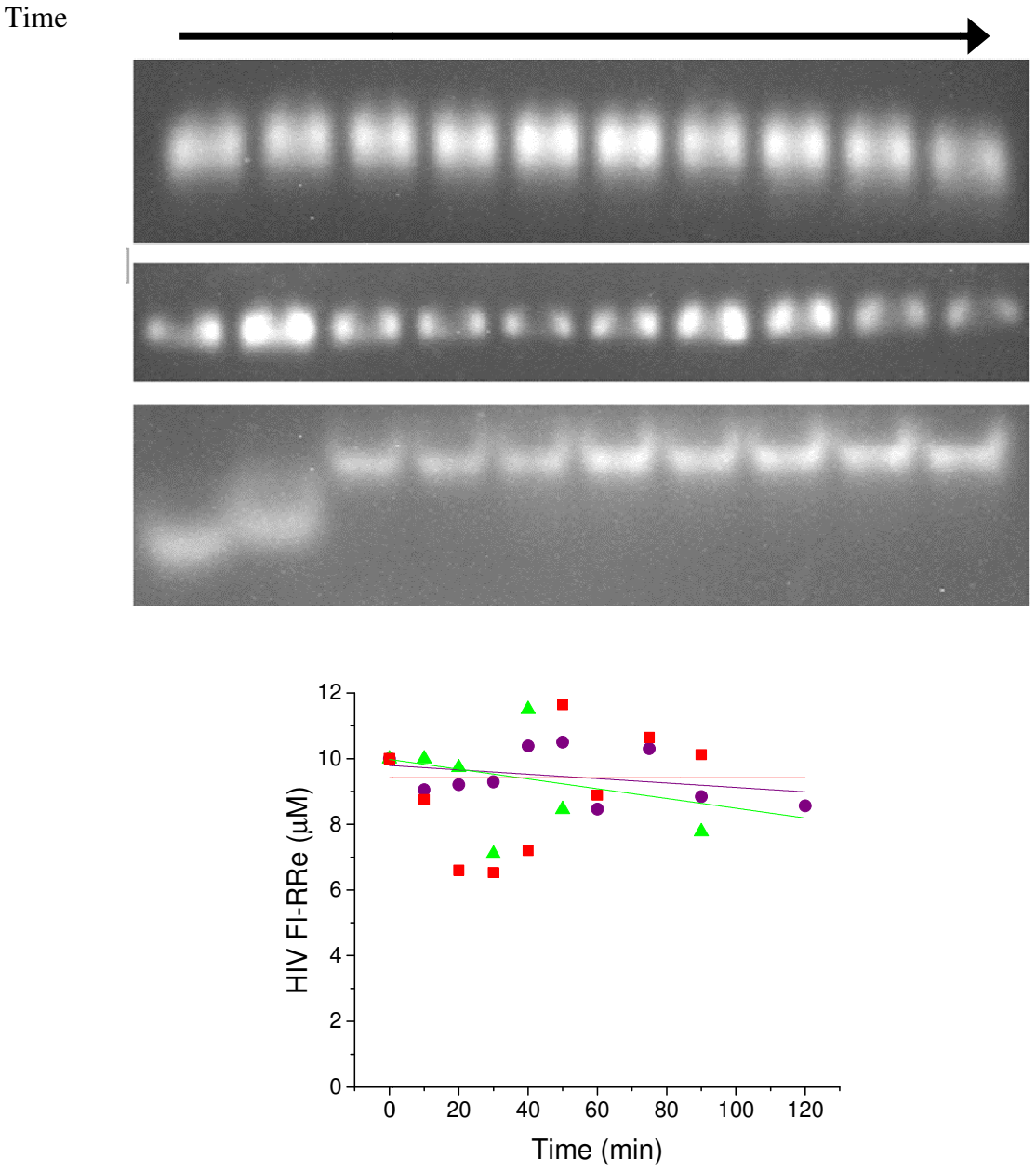

Figure SM4. Reactivity of co-reagents with Fl-HIV-RRE in the presence and absence of either **2**-Cu or **3**-Cu. Lanes from left to right: control, 10, 20, 30, 40, 50, 60, 75, 90, 120 min. (Top) RNA with co-reagents and **2**-Cu; (middle) RNA with co-reagents and **3**-Cu; (bottom) Fl-HIV-RRE with co-reagents. (Bottom) Graphical representation of the disappearance of full-length Fl-HIV RRE, **2**-Cu (purple circles), **3**-Cu (green triangles), and co-reagents only (red squares).

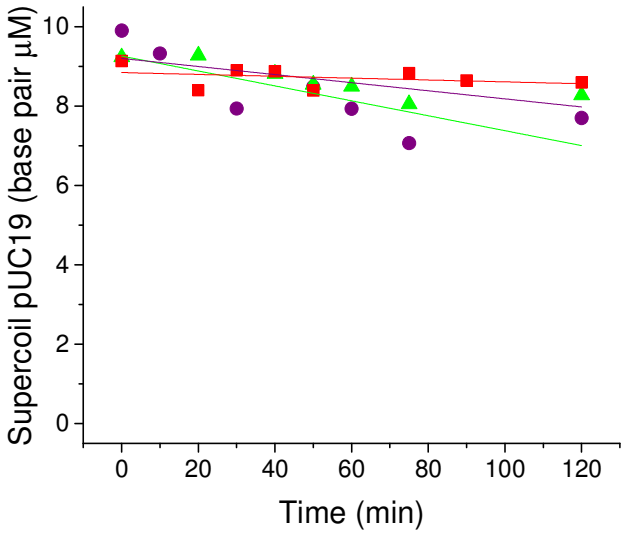

Figure SM5. Reactivity of co-reagents with 10 µM bp supercoiled pUC19 in the presence and absence of either **2**-Cu or **3**-Cu. Graphical representation of the disappearance of pUC19, **2**-Cu (purple circles), **3**-Cu (green triangles), and co-reagents only (red squares).

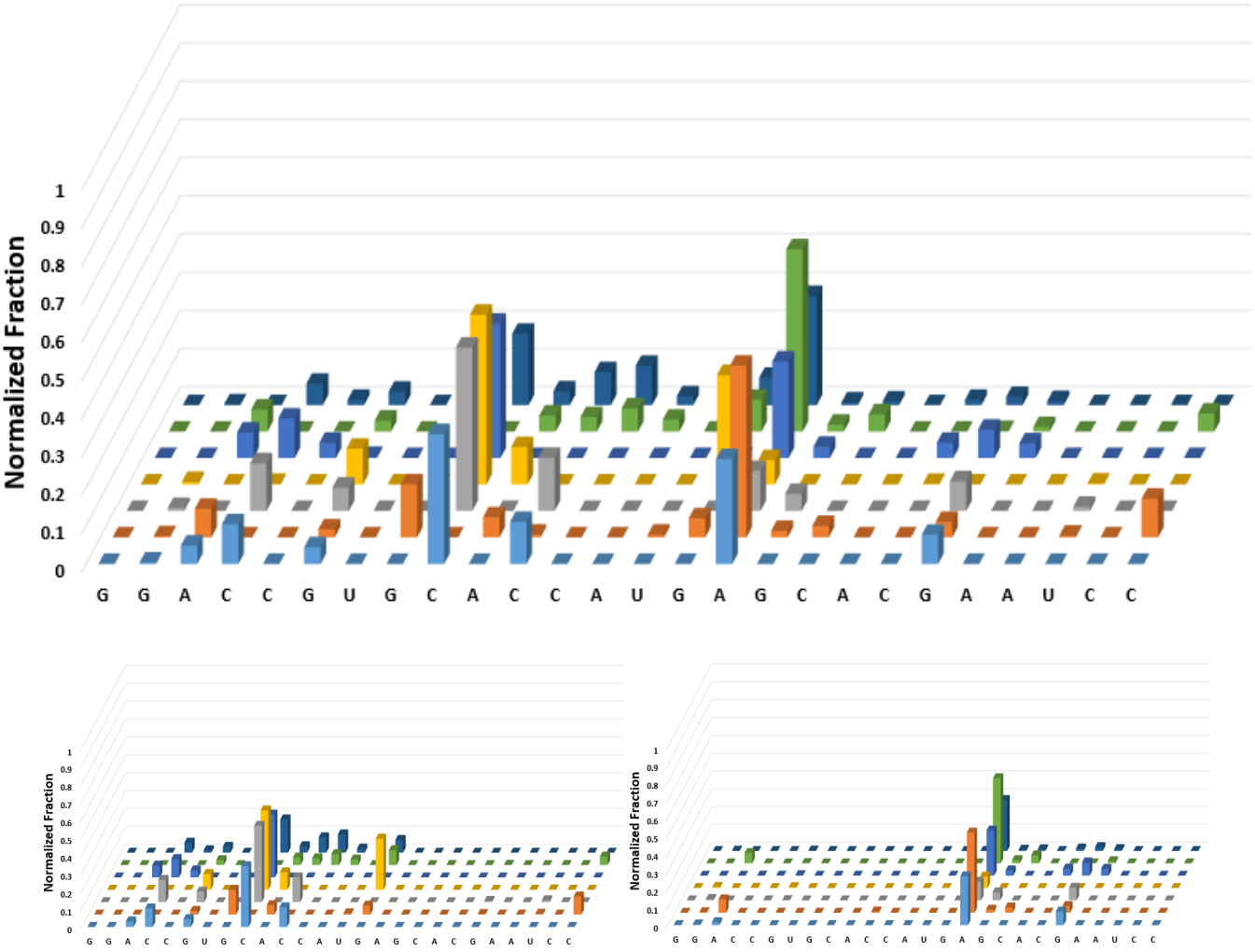

Figure SM6. (Top) Time dependence of MALDI-TOF chromatograms for reactions promoted by **2**-Cu with Fl-SLIV in the presence of coreagents. Time points from front to back include 2, 10, 20, 30, 45, 60, 90 min. The y-axis is the normalized fraction of the total intensity at each time point and does not account for mass bias. (Bottom left) Shows the contribution of the 3'-overhangs (2'/3'-phosphates, 2',3'-cyclic phosphates, 3'-OH, 3'-phosphoglycolates, 3'-enol/aldehydes, and 3'-a-B). (Bottom right) Shows the contribution of the 5'-overhangs (5'-OH/aldehydes, 5'-phosphates, and 5'-z). Figure SM9 shows structures of the different overhangs discussed.

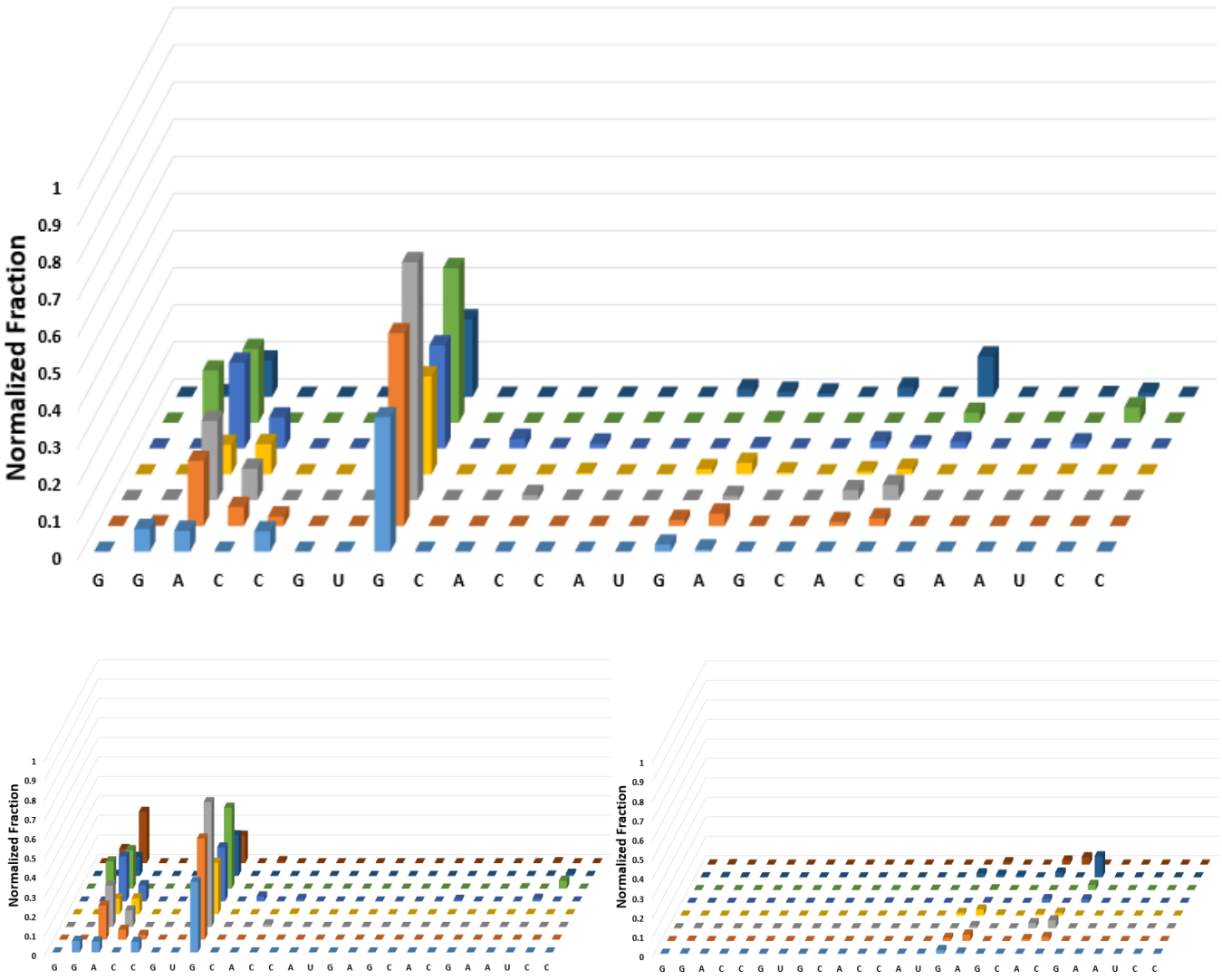

Figure SM7. (Top) Time dependence of MALDI-TOF chromatograms for reactions promoted by **3**-Cu with Fl-SLIV in the presence of coreagents. Time points from front to back include 2, 10, 20, 30, 45, 60, and 90 min. The y-axis is the normalized fraction of the total intensity at each time point and does not account for mass bias. (Bottom left) The contribution of the 3'-overhangs (2'/3'-phosphates, 2',3'-cyclic phosphates, 3'-OH, 3'-phosphoglycolates, 3'-enol/aldehydes, and 3'-a-B). (Bottom right) The contribution of the 5'-overhangs (5'-OH/aldehydes, 5'-phosphates, and 5'-z). Figure SM9 shows structures of the different overhangs discussed.

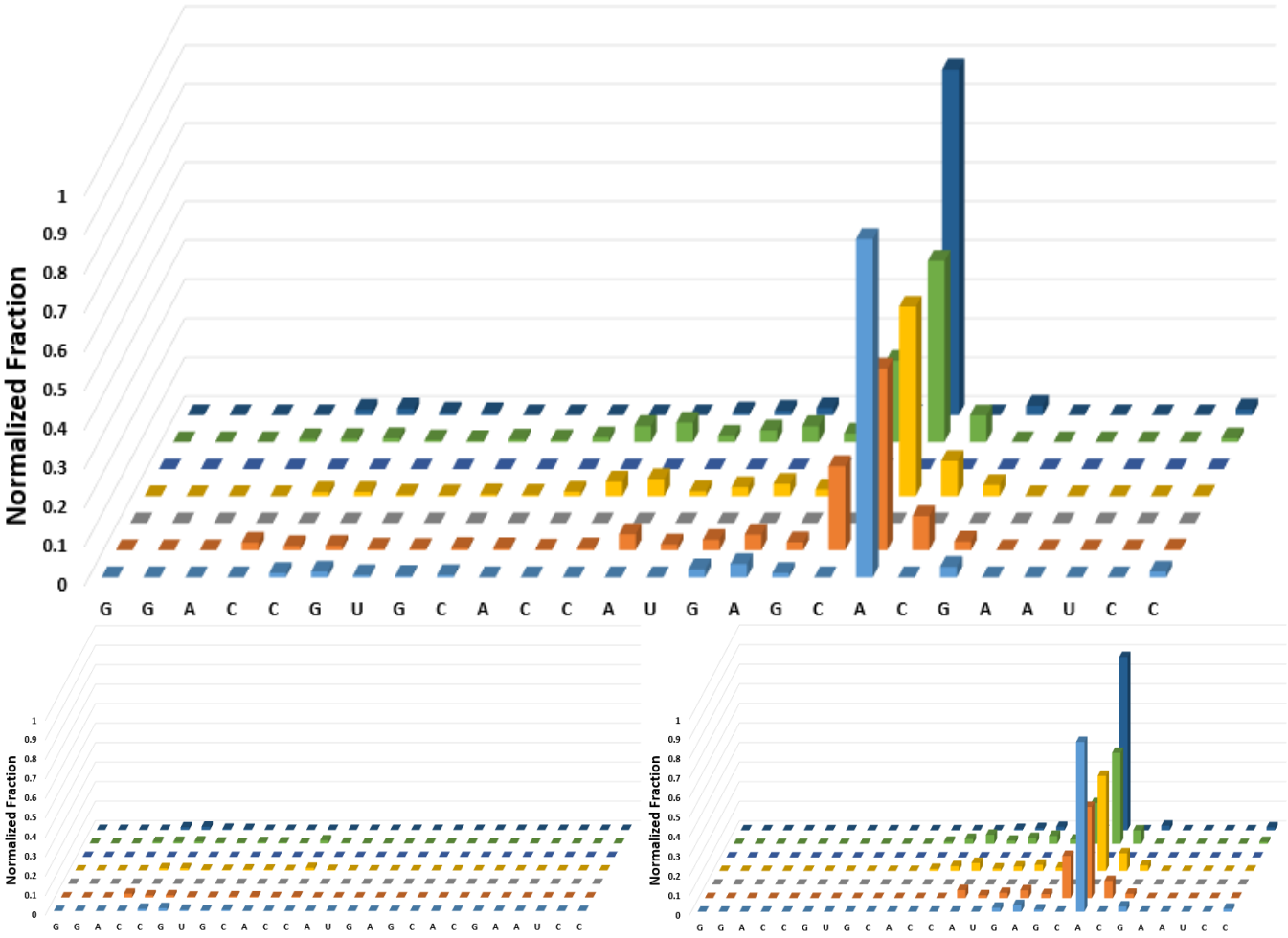

Figure SM8. (Top) Time dependence MALDI-TOF chromatogram of Fl-SLIV in the presence of coreagents. Time points from front to back include 2, 10, 20, 30, 45, 60, and 90 min. The y-axis is the normalized fraction of the total intensity at each time point and does not account for mass bias. (Bottom left) The contribution of the 3'-overhangs (2'/3'-phosphates, 2',3'-cyclic phosphates, 3'-OH, 3'-phosphoglycolates, 3'-enol/aldehydes, and 3'-a-B). (Bottom right) The contribution of the 5'-overhangs (5'-OH/aldehydes, 5'-phosphates, and 5'-z). Figure SM9 shows structures of the different overhangs discussed.

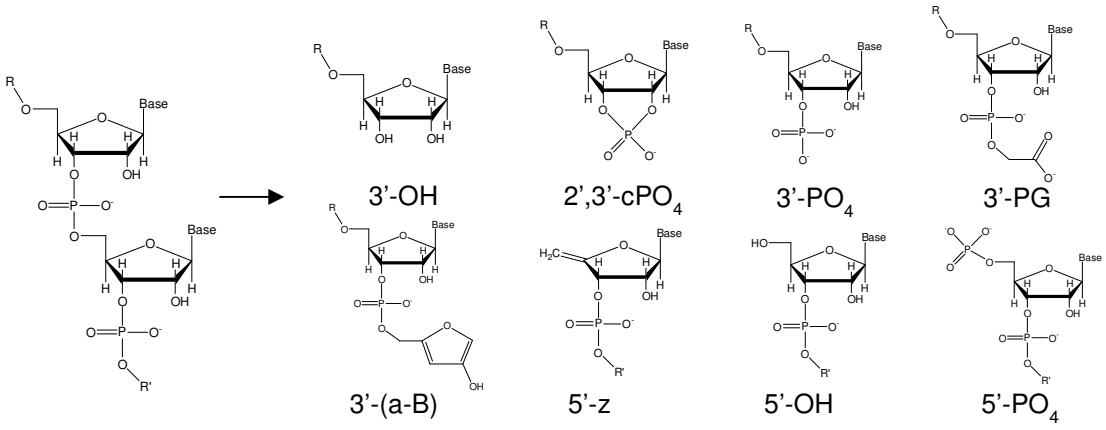

Figure SM9. Expected RNA overhangs based on known DNA cleavage pathways.

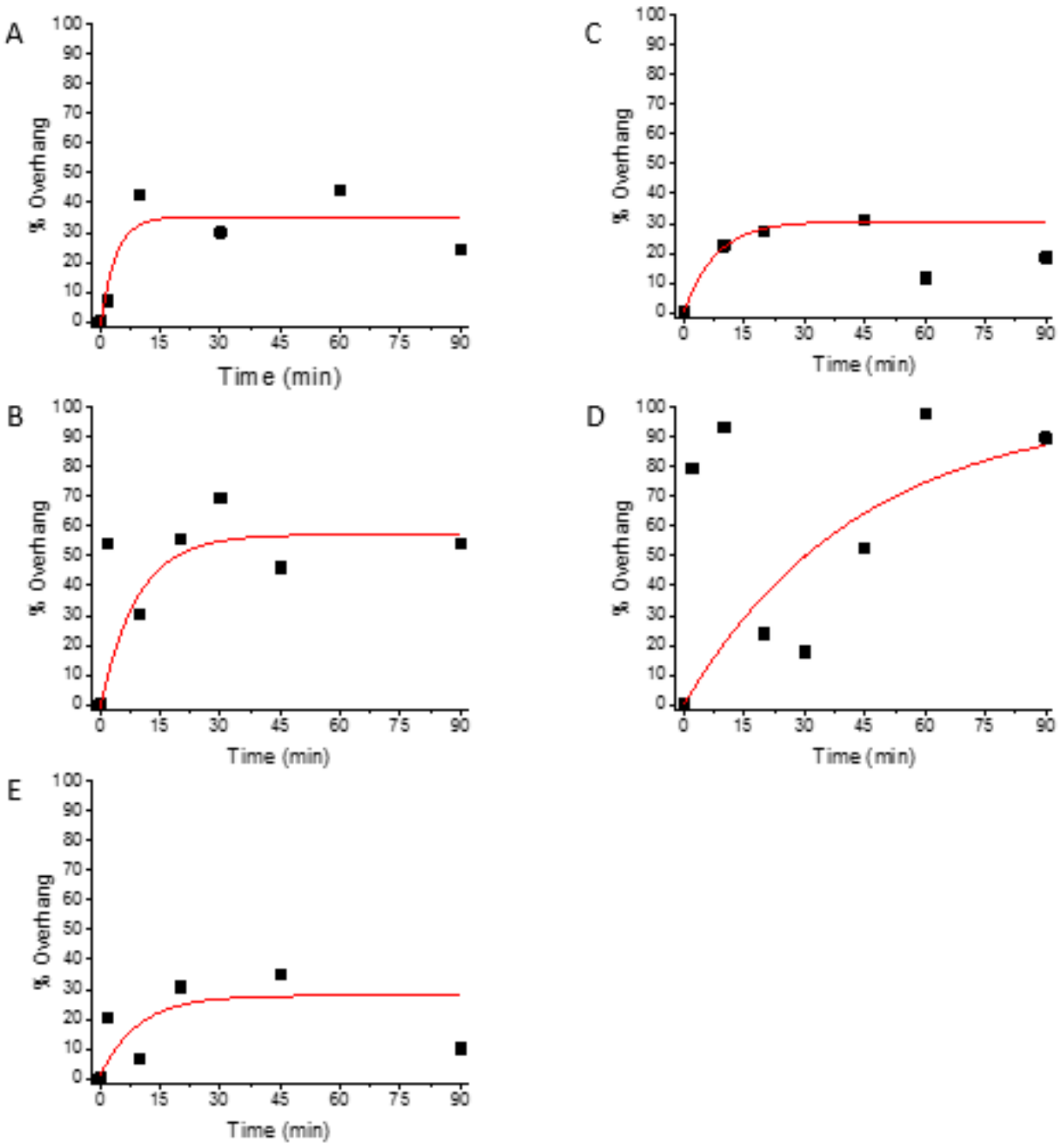

Figure SM10. Variation of overhang with time as determined for **2**-Cu and HCV SLIV from time-dependent MALDI-MS analysis; (A) 2',3'-cyclic phosphates, (B) 3'-phosphates, (C) 3'-phosphoglycolates, (D) 5'-hydroxyls, (E) 5'- phosphates.

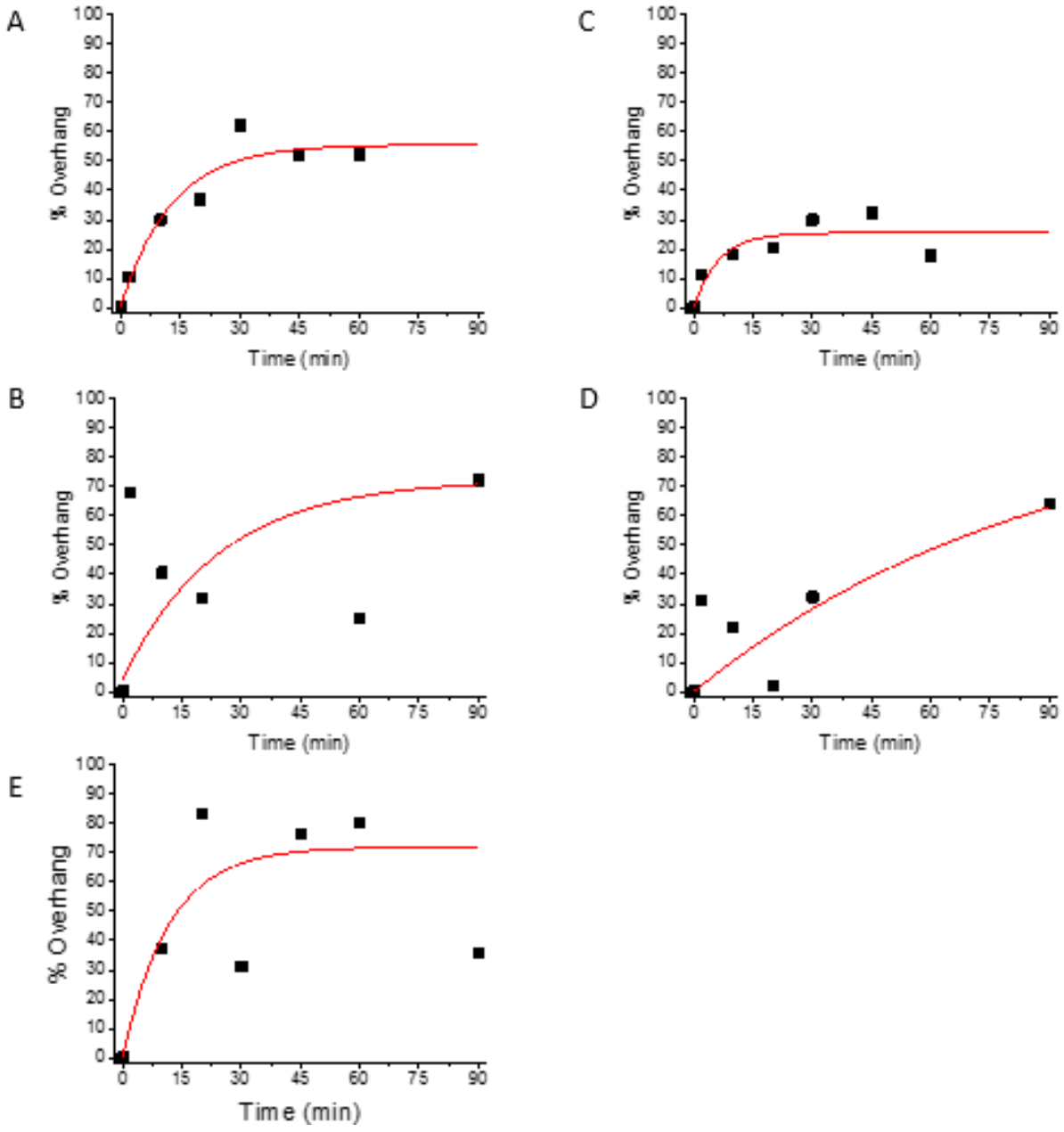

Figure SM11. Variation in overhang with time as determined for **3**-Cu and HCV SLIV from time-dependent MALDI-MS analysis; (A) 2',3'-cyclic phosphates, (B) 3'-phosphates, (C) 3'-phosphoglycolates, (D) 5'-hydroxyls, (E) 5'- phosphates.

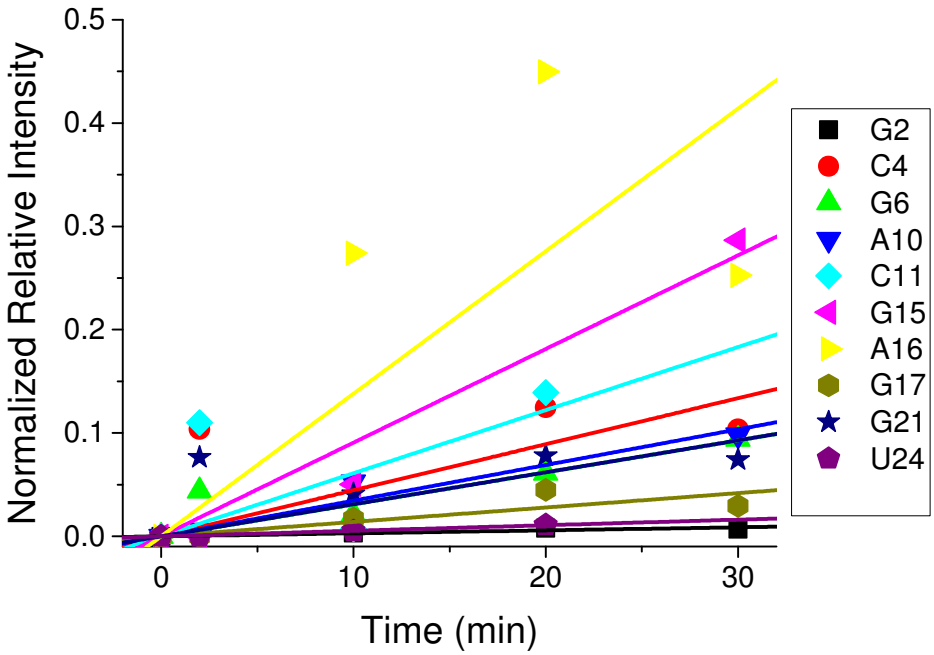

Figure SM12. Change in relative normalized intensity with time, at each overhang position, determined for the reactivity of **2**-Cu toward HCV SLIV from analysis of the time-dependence of MALDI-MS peak intensities. Linear fits to determine relative initial rates are included.

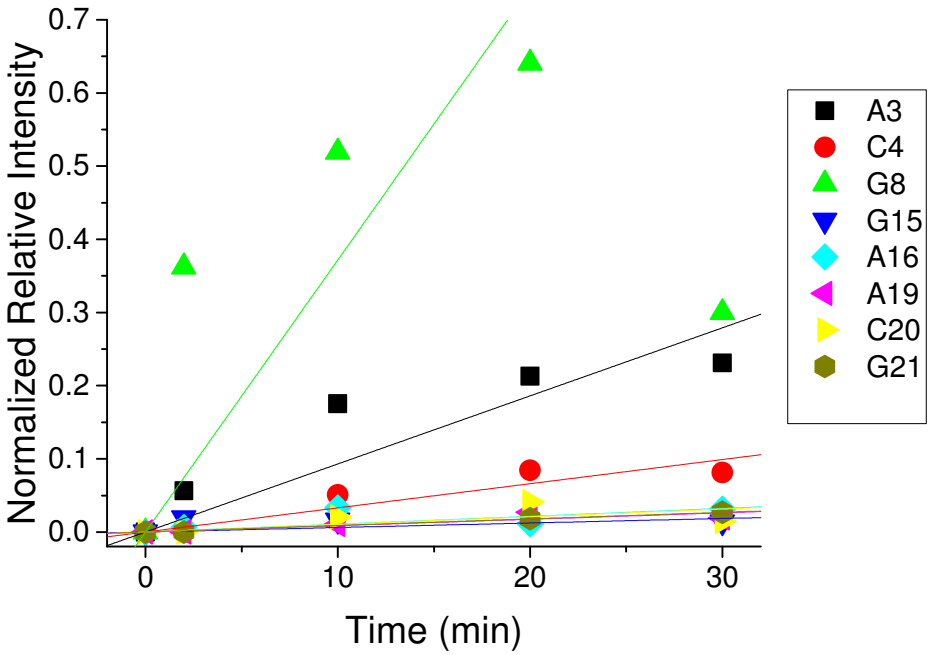

Figure SM13. Change in relative normalized intensity with time, at each overhang position, determined for the reactivity of **3**-Cu toward HCV SLIV from analysis of the time-dependence of MALDI-MS peak intensities. Linear fits to determine relative initial rates are included.

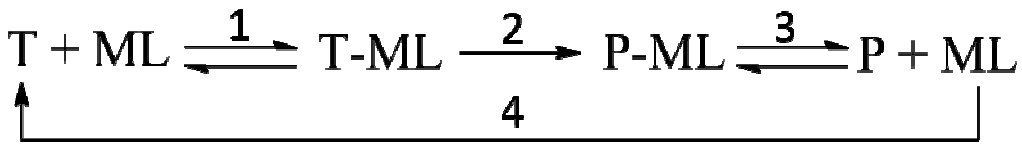

1. Binding affinity to target
2. Effectiveness in facilitating chemistry
3. Release of catalyst
4. Turnover

Figure SM14. A summary of the properties expected to contribute to and influence the effectiveness of catalytic metallodrugs. Unlike traditional drugs, the binding affinity to the target is only one of the factors that influence the effectiveness of the catalytic drug. Importantly, there needs to be a balance between the affinity to the target and the release of the therapeutic agent from the modified target.

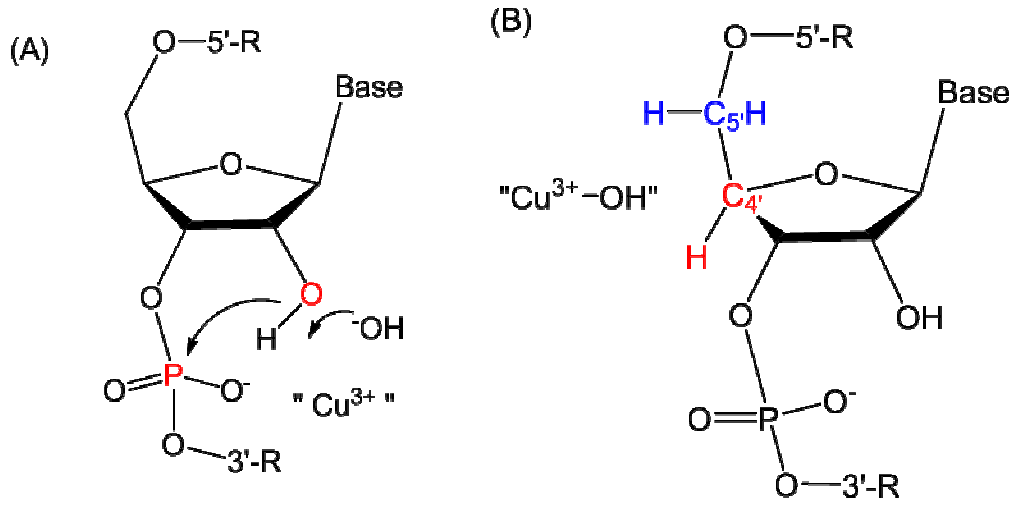

Figure SM15. Under oxidative conditions, catalysts can promote RNA cleavage chemistry either through "hydrolytic" (A) or "oxidative" (B) mechanisms promoted through the transient formation of higher valent Cu^{3+}. The illustration shows initial intermediates proposed for RNA cleavage mechanisms. The requirement for redox coreagents to effect cleavage supports the requirement for Cu^{3+} formation and transient intermediates are shown that invoke either a role as Lewis acid in a classical hydrolytic mechanism involving a cyclic phosphate ester (A), where the Cu^{3+} promotes formation of an outer or inner sphere hydroxide that deprotonates the 2'-hydroxyl and/or stabilizes the build-up of negative charge density in the transition state of cyclic phosphate ester formation; or (B), by an oxidative pathway involving a copper-associated reactive oxygen species that is positioned to mediate hydrogen abstraction from the C4' or C5' hydrogens. For the analogous reactions for oxidative cleavage of DNA, both C4'-H or C5'-H hydrogen abstraction are most common, though the oligonucleotide 3'-phosphate product can be observed for oxidative C-H scission at any ribose carbon. For RNA, the oxidative reaction (B) is suggested to most likely occur by C4'-H or C5'-H hydrogen abstraction because these hydrogens are typically the most accessible and the pathways are less compromised by the presence of the C2'-OH. Adopted from Bradford *et al.*[1]

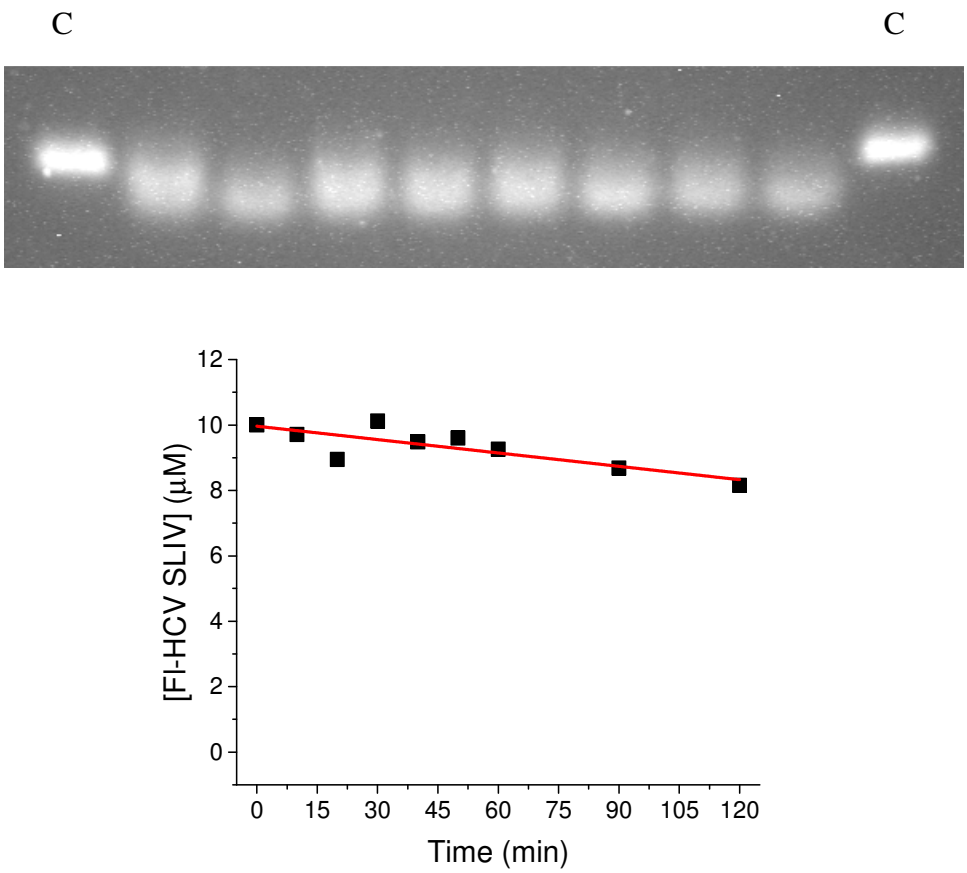

Figure SM16. Disappearance of full-length Fl-HCV-SLIV with Cu-GGH in the presence of ascorbic acid and hydrogen peroxide. The control lane (C) is shown on the on the far right and far left. The time points for each data set were (left to right) 10, 20, 30, 40, 50, 60, 90, and 120 min. Reaction conditions included 10 μM RNA and 10 μM complex with 1 mM ascorbic acid and 1 mM hydrogen peroxide. (Bottom) Graphical representation of the disappearance of the full-length Fl-HCV SLIV. Initial rate of disappearance was determined to be 13 ± 2 nM/min.

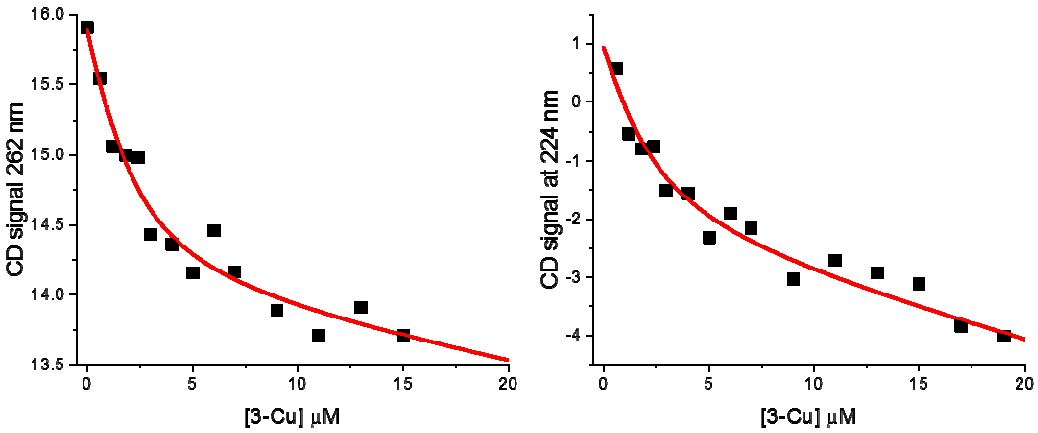

Figure SM 17. CD Titration of **3-**Cu with 2.5 µM HCV SLIV at selected wavelengths (262 nm, left and 224 nm, right). The average K_D was determined to be 1.2 ± 0.2 µM.

Table SM1. MALDI-TOF peak global assignments for each time point from the **2**-Cu promoted reaction with SLIV in the presences of co-reagents.

2 min

Theor Mass	Obsd Mass	Mass Error (ppm)	Position	Overhang	Peak Area	Normalized Peak Area
7977.89	7977.99	12.90	2	5'-OH	140.21	0.0039
1632.15	1632.07	-49.04	3	3'-phosphoglycolate	1125.06	0.0313
7632.68	7632.52	-21.40	3	5'-OH	595.55	0.0166
1975.37	1975.39	8.19	4	3'-a-B	3734.01	0.1038
2511.67	2511.55	-48.61	6	2',3'-cyclic phosphate	1577.77	0.0438
3486.24	3486.73	141.75	9	3'-phosphate	12239.36	0.3401
4178.67	4177.58	-261.49	11	3'-phosphoglycolate	3959.29	0.1100
3471.18	3470.55	-181.25	16	5'-OH	9862.97	0.2741
1937.17	1936.70	-245.01	21	5'-phosphate	2750.41	0.0764

10 min

Theor Mass	Obsd Mass	Mass Error (ppm)	Position	Overhang	Peak Area	Normalized Peak Area
8057.87	8059.70	226.69	2	5'-phosphate	108.50	0.0032
7632.68	7633.42	96.55	3	5'-OH	2558.92	0.0750
2511.67	2511.92	101.17	6	2',3'-cyclic phosphate	696.12	0.0204
6693.11	6694.94	273.32	6	5'-OH	26.40	0.0008
3163.05	3162.25	-252.23	8	2',3'-cyclic phosphate	2848.47	0.0835
3181.06	3180.47	-185.89	8	3'-phosphate	1889.24	0.0554
3815.45	3815.06	-102.18	10	3'-phosphate	1797.83	0.0527
5062.13	5060.80	-262.24	11	5'-OH	245.54	0.0072
5061.19	5060.80	-76.56	14	3'-phosphate	245.54	0.0072
5388.39	5387.54	-157.26	15	2',3'-cyclic phosphate	1714.60	0.0503
3471.18	3470.57	-175.79	16	5'-OH	15345.22	0.4498
3141.97	3142.78	258.18	17	5'-OH	585.85	0.0172
2796.76	2796.76	1.31	18	5'-OH	1026.97	0.0301
1937.17	1936.73	-227.27	21	5'-phosphate	1281.15	0.0376
7347.59	7347.30	-39.48	21	2',3'-cyclic phosphate	116.36	0.0034
8312.18	8313.68	181.00	24	2',3'-cyclic phosphate	168.98	0.0050
8860.57	8861.30	81.90	26	3'-OH	3460.01	0.1014

20 min

Theor Mass	Obsd Mass	Mass Error (ppm)	Position	Overhang	Peak Area	Normalized Peak Area
7977.89	7975.79	-263.53	2	5'-OH	170.83	0.0079
1937.33	1936.80	-274.70	4	3'-phosphoglycolate	1530.67	0.0709
1975.37	1975.83	231.98	4	3'-a-B	1164.63	0.0539
2511.67	2511.44	-89.78	6	2',3'-cyclic phosphate	1285.11	0.0595
6693.11	6692.58	-79.81	6	5'-OH	39.13	0.0018
3486.24	3486.31	21.40	9	3'-phosphate	9239.77	0.4278
4178.67	4177.79	-210.91	11	3'-phosphoglycolate	3008.07	0.1393
3453.17	3453.48	89.35	16	5'-z	2261.79	0.1047
3141.97	3141.94	-8.41	17	5'-OH	972.75	0.0450
1937.17	1936.80	-190.58	21	5'-phosphate	1530.67	0.0709
7347.59	7347.15	-60.06	21	2',3'-cyclic phosphate	153.88	0.0071
8312.18	8311.82	-43.72	24	2',3'-cyclic phosphate	238.61	0.0110

30 min

Theor Mass	Obsd Mass	Mass Error (ppm)	Position	Overhang	Peak Area	Normalized Peak Area
7977.89	7978.53	80.63	2	5'-OH	353.36	0.0070
7303.47	7302.64	-113.84	4	5'-OH	73.01	0.0014
2511.67	2511.50	-67.54	6	2',3'-cyclic phosphate	4504.17	0.0887
6693.11	6693.24	20.00	6	5'-OH	265.06	0.0052
3486.24	3486.63	111.01	9	3'-phosphate	22575.42	0.4447
3815.45	3814.63	-215.04	10	3'-phosphate	4971.40	0.0979
5388.39	5387.08	-243.77	15	2',3'-cyclic phosphate	9483.08	0.1868
5406.40	5405.03	-254.23	15	3'-phosphate	5067.30	0.0998
3453.17	3453.98	234.25	16	5'-z	3251.93	0.0641
7002.38	7002.22	-23.49	20	2',3'-cyclic phosphate	90.17	0.0018
8250.21	8250.30	11.21	24	3'-OH	129.45	0.0025

45 min

Theor Mass	Obsd Mass	Mass Error (ppm)	Position	Overhang	Peak Area	Normalized Peak Area
1632.15	1632.19	20.19	3	3'-phosphoglycolate	1332.04	0.0407
1670.19	1669.74	-270.47	3	3'-a-B	845.60	0.0258
1975.37	1975.21	-83.41	4	3'-a-B	3375.83	0.1032
7303.47	7302.32	-157.22	4	5'-OH	11.61	0.0004

2242.51	2242.32	-88.22	5	3'-phosphoglycolate	1316.72	0.0402
6693.11	6692.69	-62.89	6	5'-OH	92.58	0.0028
3486.24	3486.94	201.20	9	3'-phosphate	8455.90	0.2585
3544.28	3543.45	-233.94	9	3'-phosphoglycolate	3058.81	0.0935
3471.18	3470.37	-232.85	16	5'-OH	6458.36	0.1974
3453.17	3453.59	122.40	16	5'-z	1811.80	0.0554
3141.97	3142.72	239.85	17	5'-OH	964.61	0.0295
2242.35	2242.32	-15.53	20	5'-phosphate	1316.72	0.0402
1937.17	1936.70	-240.91	21	5'-phosphate	2426.28	0.0742
1591.96	1592.23	171.24	22	5'-phosphate	1250.02	0.0382

60 min

Theor Mass	Obsd Mass	Mass Error (ppm)	Position	Overhang	Peak Area	Normalized Peak Area
7632.68	7631.88	-104.32	3	5'-OH	4603.02	0.0577
2511.67	2511.80	49.83	6	2',3'-cyclic phosphate	2201.31	0.0276
6693.11	6693.21	15.57	6	5'OH	99.49	0.0012
3163.05	3162.45	-189.21	8	2',3'-cyclic phosphate	4503.11	0.0564
3815.45	3815.17	-72.96	10	3'-phosphate	3355.86	0.0421
4178.67	4179.35	162.37	11	3'-phosphoglycolate	3015.34	0.0378
4467.85	4467.09	-170.88	12	3'-enol/aldehyde	4856.58	0.0609
4755.02	4755.47	95.30	13	3'-phosphate	2489.12	0.0312
5388.39	5387.85	-100.48	15	2',3'-cyclic phosphate	4786.66	0.0600
5406.40	5406.55	27.71	15	3'-phosphate	1861.22	0.0233
3471.18	3470.48	-201.59	16	5'-OH	38085.95	0.4774
3141.97	3141.66	-99.17	17	5'-OH	1451.17	0.0182
2796.76	2796.54	-80.15	18	5'-OH	3562.47	0.0447
6367.99	6368.51	82.30	18	2',3'-cyclic phosphate	24.28	0.0003
7347.59	7348.36	104.73	21	2',3'-cyclic phosphate	98.34	0.0012
1591.96	1592.14	111.97	22	5'-phosphate	954.51	0.0120
8250.21	8249.58	-76.27	24	3'-OH	49.97	0.0006
8860.57	8861.67	123.73	26	3'-OH	3780.34	0.0474

90 min

Theor Mass	Obsd Mass	Mass Error (ppm)	Position	Overhang	Peak Area	Normalized Peak Area
7977.89	7977.80	-10.93	2	5'-OH	114.20	0.0016
1937.33	1936.89	-229.50	4	3'-phosphoglycolate	1531.99	0.0218
1975.37	1975.36	-5.40	4	3'-a-B	1326.77	0.0189

1861.28	1861.28	-1.64	4	2',3'-cyclic phosphate	587.69	0.0083
1879.29	1879.32	16.14	4	3'-phosphate	510.07	0.0072
2242.51	2242.21	-134.79	5	3'-phosphoglycolate	972.87	0.0138
2511.67	2511.56	-45.26	6	2',3'-cyclic phosphate	2326.01	0.0330
6693.11	6691.69	-212.16	6	5'-OH	152.38	0.0022
3163.05	3162.11	-295.64	8	2',3'-cyclic phosphate	2625.14	0.0373
3486.24	3487.02	224.06	9	3'-phosphate	13143.42	0.1867
3815.45	3815.02	-113.38	10	3'-phosphate	2531.31	0.0360
4178.67	4178.21	-110.32	11	3'-phosphoglycolate	2673.34	0.0380
4120.63	4120.67	10.58	11	3'-phosphate	1973.55	0.0280
4102.62	4102.38	-57.86	11	2',3'-cyclic phosphate	1431.46	0.0203
4483.85	4484.92	238.94	12	3'-phosphoglycolate	3238.32	0.0460
4425.81	4426.31	113.35	12	3'-phosphate	2507.36	0.0356
4407.80	4407.28	-117.07	12	2',3'-cyclic phosphate	1509.98	0.0215
4755.02	4755.02	-0.86	13	3'-phosphate	1650.74	0.0235
5388.39	5387.63	-140.48	15	2',3'-cyclic phosphate	2622.08	0.0373
5406.40	5405.71	-128.34	15	3'-phosphate	2429.07	0.0345
3471.18	3470.39	-227.59	16	5'-OH	20089.61	0.2854
3141.97	3141.64	-103.54	17	5'-OH	493.55	0.0070
2796.76	2796.41	-126.11	18	5'-OH	698.09	0.0099
2242.35	2242.21	-62.11	20	5'-phosphate	972.87	0.0138
1937.17	1936.89	-145.38	21	5'-phosphate	1531.99	0.0218
1511.98	1511.99	3.34	22	5'-OH	740.56	0.0105

Table SM2. MALDI-TOF peak global assignments for each time point from the **3**-Cu promoted reaction with SLIV in the presences of co-reagents

2 min

Theor Mass	Obsd Mass	Mass Error (ppm)	Position	Overhang	Peak Area	Normalized Peak Area
1632.15	1632.10	-35.31	3	3'-phosphoglycolate	520.36	0.0593
7632.68	7631.31	-179.58	3	5'-OH	118.81	0.0021
1975.37	1975.07	-152.69	4	3'-a-B	524.76	0.0564
2511.67	2511.23	-176.92	6	2',3'-cyclic phosphate	350.47	0.0546
6693.11	6692.87	-36.16	6	5'-OH	14.14	0.0003
3486.24	3485.91	-94.18	9	3'-phosphate	3196.97	0.3624
3453.17	3453.51	99.10	16	5'-z	1328.08	0.0194
3141.97	3142.39	135.22	17	5'-OH	367.11	0.0064

10 min

Theor Mass	Obsd Mass	Mass Error (ppm)	Position	Overhang	Peak Area	Normalized Peak Area
7632.68	7634.41	226.50	3	5'-OH	185.77	0.0020
1937.33	1937.12	-107.78	4	3'-phosphoglycolate	1880.90	0.0893
1975.37	1975.67	150.64	4	3'-a-B	1719.87	0.0862
2242.51	2242.12	-175.72	5	3'-phosphoglycolate	977.80	0.0509
2511.67	2511.71	14.22	6	2',3'-cyclic phosphate	601.53	0.0249
6693.11	6693.76	96.78	6	5'-OH	33.53	0.0004
3486.24	3485.38	-247.77	9	3'-phosphate	6557.81	0.3133
3468.23	3469.03	231.81	9	2',3'-cyclic phosphate	4843.92	0.2060
3453.17	3453.09	-21.87	16	5'-z	1465.26	0.0164
3123.96	3124.79	265.15	17	5'-z	1524.76	0.0173
3141.97	3141.83	-43.31	17	5'-OH	1471.02	0.0159
2242.35	2242.12	-103.04	20	5'-phosphate	977.80	0.0106
1937.17	1937.12	-23.65	21	5'-phosphate	1880.90	0.0206

20 min

Theor Mass	Obsd Mass	Mass Error (ppm)	Position	Overhang	Peak Area	Normalized Peak Area
7632.68	7632.88	26.39	3	5'-OH	202.60	0.0017
1937.33	1937.30	-18.65	4	3'-phosphoglycolate	4773.50	0.1112
1975.37	1975.35	-11.27	4	3'-a-B	4393.78	0.1017
2242.51	2241.85	-297.73	5	3'-phosphoglycolate	3223.34	0.0845
3468.23	3468.62	112.48	9	2',3'-cyclic phosphate	17997.33	0.3371

3486.24	3485.22	-291.90	9	3'-phosphate	12981.06	0.3036
4407.80	4407.93	29.74	12	2',3'-cyclic phosphate	472.44	0.0134
4738.94	4738.30	-135.98	12	5'-z	37.14	0.0003
4737.01	4738.30	271.39	13	2',3'-cyclic phosphate	37.14	0.0011
3123.96	3124.55	189.18	17	5'-z	1268.99	0.0114
2242.35	2241.85	-225.06	20	5'-phosphate	3223.34	0.0269
1937.17	1937.30	65.50	21	5'-phosphate	4773.50	0.0410

30 min

Theor Mass	Obsd Mass	Mass Error (ppm)	Position	Overhang	Peak Area	Normalized Peak Area
8323.10	8323.09	-1.25	1	5'-OH	7.29	0.0001
1937.33	1937.54	108.48	4	3'-phosphoglycolate	1563.45	0.0793
2242.51	2242.25	-118.53	5	3'-phosphoglycolate	890.95	0.0491
2280.55	2280.21	-150.43	5	3'-a-B	922.51	0.0321
6693.11	6693.12	1.99	6	5'-OH	22.62	0.0002
3468.23	3468.28	13.70	9	2',3'-cyclic phosphate	4041.27	0.2637
4737.01	4737.20	40.55	13	2',3'-cyclic phosphate	42.51	0.0038
3453.17	3452.17	-288.85	16	5'-z	1452.24	0.0139
3141.97	3141.23	-234.92	17	5'-OH	1978.76	0.0181
3123.96	3124.30	108.85	17	5'-z	1344.91	0.0130
2796.76	2796.26	-178.05	18	5'-OH	603.06	0.0056
2242.35	2242.25	-45.85	20	5'-phosphate	890.95	0.0083
1937.17	1937.54	192.64	21	5'-phosphate	1563.45	0.0147
8555.39	8555.19	-23.87	25	3'-OH	21.95	0.0014

45 min

Theor Mass	Obsd Mass	Mass Error (ppm)	Position	Overhang	Peak Area	Normalized Peak Area
1937.33	1937.78	228.78	4	3'-phosphoglycolate	2177.68	0.1270
1975.37	1975.37	-1.77	4	3'-a-B	1757.59	0.1042
2242.51	2241.99	-234.21	5	3'-phosphoglycolate	1267.00	0.0838
3468.23	3467.59	-185.72	9	2',3'-cyclic phosphate	3280.43	0.2776
4102.62	4103.11	120.12	11	2',3'-cyclic phosphate	221.01	0.0259
4738.94	4737.92	-216.03	12	5'-z	110.85	0.0017
4737.01	4737.92	191.31	13	2',3'-cyclic phosphate	110.85	0.0133
3123.96	3123.78	-58.31	17	5'-z	269.47	0.0042

2242.35	2241.99	-161.54	20	5'-phosphate	1267.00	0.0193
7347.59	7345.53	-280.74	21	2',3'-cyclic phosphate	72.67	0.0089
1634.00	1633.99	-6.48	22	5'-enol/aldehyde	1167.88	0.0183
8617.36	8616.23	-131.10	25	2',3'-cyclic phosphate	114.83	0.0141

60 min

Theor Mass	Obsd Mass	Mass Error (ppm)	Position	Overhang	Peak Area	Normalized Peak Area
7977.89	7977.38	-63.76	2	5'-OH	32.03	0.0003
1632.15	1632.35	121.09	3	3'-phosphoglycolate	2225.07	0.1404
1879.29	1879.12	-92.69	4	3'-phosphate	1335.56	0.1984
3468.23	3467.21	-293.43	9	2',3'-cyclic phosphate	4800.17	0.4161
4104.55	4104.79	59.63	14	5'-z	189.43	0.0020
3123.96	3123.29	-214.84	17	5'-z	392.07	0.0042
7347.59	7348.09	67.83	21	2',3'-cyclic phosphate	4.16	0.0006
1591.96	1592.36	252.28	22	5'-phosphate	2556.38	0.0268
8250.21	8249.41	-97.16	24	3'-OH	35.40	0.0029
8860.57	8862.18	181.59	26	3'-OH	494.06	0.0411

90 min

Theor Mass	Obsd Mass	Mass Error (ppm)	Position	Overhang	Peak Area	Normalized Peak Area
7977.89	7975.88	-251.96	2	5'-OH	19.59	0.0004
1574.11	1573.96	-93.43	3	3'-phosphate	69.55	0.0059
7632.68	7631.27	-184.23	3	5'-OH	70.69	0.0016
1975.37	1974.88	-246.81	4	3'-a-B	1611.27	0.0756
1879.29	1879.12	-89.18	4	3'-phosphate	246.52	0.0212
1861.28	1860.89	-209.92	4	2',3'-cyclic phosphate	15.03	0.0013
3486.24	3486.32	24.01	9	3'-phosphate	2375.82	0.2089
4737.01	4737.26	52.10	13	2',3'-cyclic phosphate	6.18	0.0005
3471.18	3470.35	-238.77	16	5'-OH	920.37	0.0210
3141.97	3142.23	81.19	17	5'-OH	600.52	0.0140
2796.76	2796.30	-166.20	18	5'-OH	392.75	0.0093
2242.35	2241.68	-297.58	20	5'-phosphate	977.70	0.0251
1511.98	1512.18	135.29	22	5'-OH	2908.68	0.0694
1591.96	1592.30	214.05	22	5'-phosphate	1497.62	0.0394
8555.39	8554.41	-113.98	25	3'-OH	28.33	0.0024
8860.57	8862.00	161.60	26	3'-OH	134.50	0.0114

Reference.

1. Bradford, S. S.; Ross, M. J.; Fidai, I.; Cowan, J. A., Insight into the recognition, binding, and reactivity of catalytic metallodrugs targeting stem loop IIb of hepatitis C IRES RNA. *ChemMedChem* **2014,** *9* (6), 1275-85.